

**FULL NLO MASSIVE GAUGE BOSON
PAIR PRODUCTION AT THE LHC**Julien Baglio^{1 a}, Le Duc Ninh^{1,2} and Marcus M. Weber³¹ *Institut für Theoretische Physik, Karlsruher Institut für Technologie,
Wolfgang Gaede Strasse 1, Karlsruhe DE-76131, Germany*² *Institute of Physics, Vietnam Academy of Science and Technology,
10 Dao Tan, Ba Dinh, Hanoi, Vietnam*³ *Max-Planck-Institut für Physik (Werner-Heisenberg-Institut),
München D-80805, Germany*

Electroweak gauge boson pair production is a very important process at the LHC as it probes the non-abelian structure of electroweak interactions and is a background process for many searches. We present full next-to-leading order predictions for the production cross sections and distributions of on-shell massive gauge boson pair production in the Standard Model, including both QCD and electroweak corrections. The hierarchy between the ZZ , WW and WZ channels, observed in the transverse momentum distributions, will be analyzed. We will also present a comparison with experimental data for the total cross sections including a study of the theoretical uncertainties.

1 Introduction

Since the beginning of LHC operations in 2010, there have been numerous gauge boson pair measurements at 7 and 8 TeV, in particular looking for signs of new physics via anomalous couplings^{1,2}. It is indeed crucial to test the non-abelian structure of the electroweak (EW) sector of the Standard Model (SM) as new physics effects could modify this structure. When added to the fact that gauge boson pair production is an important background in the search for the Higgs boson, this triggers precise predictions on the theoretical side.

The QCD next-to-leading order (NLO) corrections have been known for decades^{3,4,5}. A full next-to-next-to-leading order (NNLO) QCD calculation is not yet available but some approximate results have been released in the past few months, for example in the WW production⁶. NLO EW corrections, known for a long time in the high energy approximation^{7,8,9}, have been fully calculated only recently^{10,11,12} including photon-quark induced processes¹².

We present full NLO predictions for the total cross sections and the differential distributions, including both QCD and EW effects. In particular the hierarchy that is observed in the p_T distributions between the ZZ , WW and WZ channels is explained thanks to soft gauge boson approximation. A comparison with experimental data including theoretical uncertainties is also given. More details can be found in Ref.¹².

^aspeaker

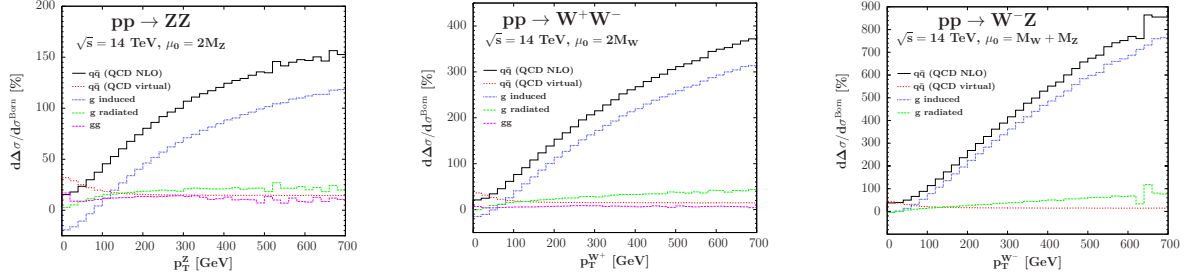


Figure 1: Z (left), W^+ (middle) and W^- (right) transverse momentum distributions (in GeV) of the NLO QCD corrections (in %) in $\sigma(pp \rightarrow ZZ, WW, W^-Z)$, respectively.

2 Overview of the calculation

The well-known QCD NLO corrections to $q\bar{q}' \rightarrow VV'$ that were calculated a while ago^{3,4,5} have been recalculated as well as the gluon fusion channel that is formally a NNLO contribution. The NLO EW corrections include not only the virtual and real photon emission corrections to $q\bar{q}'$ channels but also the photon–quark induced channels, the latter not being considered in Refs.^{10,11}. The NLO corrections to photon–photon initial state in the WW channel were also incorporated. We used the MRST2004QED PDF set¹³ to account for the photon PDF. The relevant EW parameters are renormalized in the on–shell scheme.

In order to deal with infrared singularities we used dimensional regularization and mass regularization schemes. The two calculations are in excellent agreement. The Catani-Seymour dipole subtraction method¹⁴ is used to combine the virtual and real corrections. We also cross-checked the results with the phase-space slicing method¹⁵. We performed independent calculations with the help of automated tools: the FeynArt/FormCalc¹⁶ suite to generate one-loop amplitudes. The one-loop integrals are calculated with the in-house library LoopInts, which agrees with the program LoopTools^{16,17}. MadGraph and HELAS routines are also used to calculate tree-level amplitudes. Further details about the calculation and the precise definitions of the various contributions discussed in the next section can be found in Ref.¹².

3 Hierarchy of radiative corrections

We present some selected results for the differential distributions at the LHC at 14 TeV, using the MRST2004QED PDF set and $\alpha_s(M_Z^2) = 0.1190$. The factorization and renormalization scales are both equal to $M_V + M_{V'}$. We apply no cuts at the level of the on-shell W^\pm and Z , since these will decay. It can be seen in Fig. 1 that the QCD corrections are driven by the gluon-quark induced processes (dotted blue lines) with a large correction at high p_T driven by leading-logarithmic terms proportional to $\alpha_s \log^2(M_V^2/p_T^2)$. This is explained by the large gluon PDF and soft gauge boson emission and has been noticed for quite a while^{4,5} but the hierarchy $\delta_{ZZ}^{\text{QCD}} \simeq \frac{1}{3}\delta_{WW}^{\text{QCD}} \simeq \frac{1}{6}\delta_{W^-Z}^{\text{QCD}}$ with $\delta_{ZZ}^{\text{QCD}} \simeq 120\%$, clearly visible on Fig. 1, was not well understood.

The same hierarchy is also observed in the EW corrections as displayed in Fig. 2 (left-handed and middle figures). This hierarchy is much more pronounced than for the QCD case, with $\delta_{ZZ}^{\text{EW}} \simeq \frac{1}{90}\delta_{WW}^{\text{EW}} \simeq \frac{1}{190}\delta_{W^-Z}^{\text{EW}}$ and $\delta_{ZZ}^{\text{EW}} \simeq 0.3\%$. The virtual Sudakov effect in the $q\bar{q}' \rightarrow VV'$ is clearly visible (dashed red lines) and has been also discussed in Ref.^{10,11}.

The hierarchies between the ZZ , WW and WZ channels in both QCD and EW radiative corrections share some common features. They are effects of the dominant double-logarithmic terms in the gluon-quark and photon-quark induced processes, in which the non-abelian structure of the theory, the different couplings strengths and PDF effects play a role. The analytical approximations using soft gauge boson emission from a quark-gauge boson final state, presented in Ref.¹², reproduce this hierarchy even if they are off by a factor of two at $p_T \simeq 700$ GeV. It

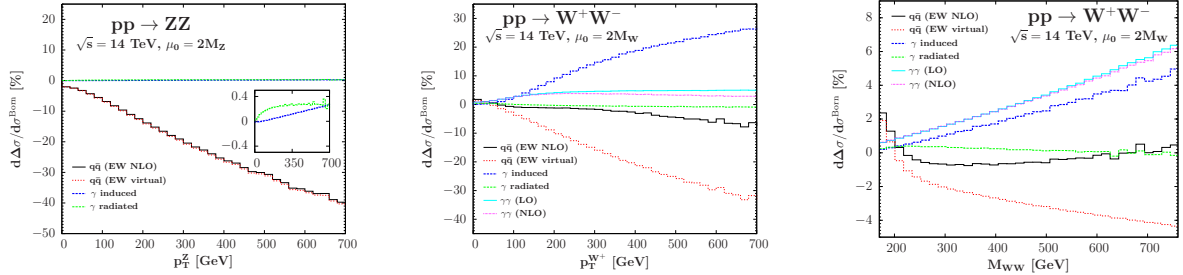


Figure 2: Z (left) and W^+ (middle) transverse momentum as well as M_{WW} invariant mass (right) distributions (in GeV) of the NLO EW corrections (in %), in $\sigma(pp \rightarrow ZZ, WW, W^-Z)$, respectively.

has been checked that they coincide with the full result at much higher p_T , thereby validating the approximation. In the case of the EW corrections, the γq processes are further enhanced by a t -channel massive gauge boson exchange, explaining the huge enhancement of the EW corrections in the WW and WZ channels compared to the ZZ channel. It compensates or even overcompensates the virtual Sudakov effect in the WW and WZ channels, making the photon-quark induced processes absolutely necessary for the full NLO EW calculation. The right-handed side of Fig. 2 shows the importance of the diphoton subprocess in the WW invariant mass distribution where it is the leading EW effect.

4 Total cross sections and comparison with experimental data

We have calculated the total cross sections fully at NLO and compared with the most up-to-date ATLAS and CMS results from HEP-EPS 2013 Conference. This is an update of our previous results¹². In order to account for the EW corrections using modern PDF sets such as the MSTW set¹⁸, we rescaled our NLO QCD predictions calculated with modern sets by a factor δ^{EW} calculated with MRST2004QED including the photon PDF: $\delta^{\text{EW}} = \sigma_{\text{QCD+EW}}^{\text{NLO}} / \sigma_{\text{QCD}}^{\text{NLO}}$. Recently the NNPDF Collaboration has released a new set including also a photon PDF¹⁹ and we have checked at the level of the total cross section that the ratio δ^{EW} does not change significantly by trading MRST2004QED with NNPDF2.3QED.

A detailed study of the theoretical uncertainties affecting the predictions has been performed. We calculated the scale uncertainty with the factorization and renormalization scales varied in the interval $\frac{1}{2}\mu_0 \leq \mu_R = \mu_F \leq 2\mu_0$ where the central scale is $\mu_0 = M_V + M_{V'}$. We used the MSTW2008 90%CL set to calculate the correlated PDF+ α_s uncertainty. The parametric uncertainties coming from the experimental errors on M_W and M_Z are negligible. The results are presented in Fig. 3 and are similar in the three different channels. We obtain $\delta^{\text{EW}} \approx 0.97, 1.00, 1.01$ for the ZZ, WZ, WW channels respectively. The scale uncertainty amounts to $\simeq +3\% / -2\%$ at 7 TeV, two times less at 33 TeV. The PDF+ α_s uncertainty is of the order of $\pm 4\%$.

We have combined the scale and PDF+ α_s into the overall theoretical uncertainty of the total cross section and compared with experimental data, as displayed in Fig. 4. We found a total uncertainty $\sim +7\% / -6\%$ at 7 and 8 TeV, slightly less at 33 TeV, in all three channels. The comparison with ATLAS and CMS results is good, in particular in the ZZ and WZ channels. In the WW channel, there is a 1σ excess at 7 TeV and a 1.8σ excess at 8 TeV. As estimated in Ref.¹² and confirmed by the results in Ref.⁶ a full NNLO calculation is not expected to account for this deviation.

Acknowledgments

J.B. would like to thank the organizers for the very nice atmosphere of the conference. This work is supported by the Deutsche Forschungsgemeinschaft via the Sonderforschungsbereich/Transregio



Figure 3: The scale uncertainty in $\sigma(pp \rightarrow ZZ)$ at the LHC (left) and the PDF/PDF+ α_s uncertainty in $\sigma(pp \rightarrow WW)$ (right), in pb, as a function of the center-of-mass energy (in TeV). In the inserts deviations from the central predictions are shown.

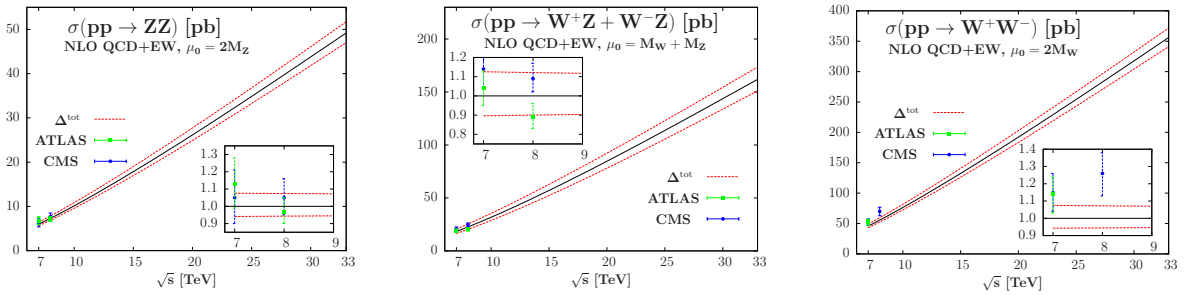


Figure 4: The NLO QCD+EW total cross section (in pb) of the processes $pp \rightarrow ZZ$ (left), $pp \rightarrow W^+Z + W^-Z$ (middle) and $pp \rightarrow WW$ (right) at the LHC as a function of the center-of-mass energy (in TeV) including the total theoretical uncertainty. The insert shows the relative deviation from the central cross sections, and the experimental data points are also displayed on the main figures.

SFB/TR-9 Computational Particle Physics.

1. ATLAS Collaboration, G. Aad *et al.*, (2012), arXiv:1210.2979.
2. CMS Collaboration, S. Chatrchyan *et al.*, Phys.Lett. **B721**, 190 (2013), arXiv:1301.4698.
3. J. Ohnemus, Phys.Rev. **D44**, 3477 (1991).
4. S. Frixione, Nucl.Phys. **B410**, 280 (1993).
5. J. Ohnemus, Phys.Rev. **D50**, 1931 (1994), hep-ph/9403331.
6. S. Dawson, I. M. Lewis, and M. Zeng, (2013), arXiv:1307.3249.
7. E. Accomando, A. Denner, and S. Pozzorini, Phys.Rev. **D65**, 073003 (2002), hep-ph/0110114.
8. E. Accomando, A. Denner, and A. Kaiser, Nucl.Phys. **B706**, 325 (2005), hep-ph/0409247.
9. E. Accomando, A. Denner, and C. Meier, Eur.Phys.J. **C47**, 125 (2006), hep-ph/0509234.
10. A. Bierweiler, T. Kasprzik, H. Kühn, and S. Uccirati, JHEP **1211**, 093 (2012), arXiv:1208.3147.
11. A. Bierweiler, T. Kasprzik, and J. H. Kühn, (2013), arXiv:1305.5402.
12. J. Baglio, L. D. Ninh, and M. M. Weber, (2013), arXiv:1307.4331.
13. A. Martin, R. Roberts, W. Stirling, and R. Thorne, Eur.Phys.J. **C39**, 155 (2005), hep-ph/0411040.
14. S. Catani and M. Seymour, Nucl.Phys. **B485**, 291 (1997), hep-ph/9605323.
15. U. Baur, S. Keller, and D. Wackerroth, Phys.Rev. **D59**, 013002 (1998), hep-ph/9807417.
16. T. Hahn and M. Perez-Victoria, Comput. Phys. Commun. **118**, 153 (1999).
17. G. van Oldenborgh, Comput.Phys.Commun. **66**, 1 (1991).
18. A. Martin, W. Stirling, R. Thorne, and G. Watt, Eur.Phys.J. **C63**, 189 (2009), arXiv:0901.0002.
19. The NNPDF Collaboration, R. D. Ball *et al.*, (2013), arXiv:1308.0598.